

DR. THOMAS M. LILLESAND
State University of New York
College of Environmental Science and Forestry
Syracuse, New York 13210
DR. FRANK L. SCARPACE
DR. JAMES L. CLAPP
University of Wisconsin
Madison, Wisconsin 53706

Water Quality in Mixing Zones

Photometry applied to aerial photographs, supported by a limited amount of ground sampling, can be used to measure and delineate waste distributions as reliably and in more detail than conventional surface measuring techniques.

INTRODUCTION

PROBLEM IDENTIFICATION

ASSOCIATED with the rapid and continuous industrial growth of the last two decades has been excessive degradation of water

chemical, physical and biological integrity of U.S. surface waters. In order to achieve this objective, it is a national goal that the discharge of pollutants into navigable waters be eliminated by 1985.

Although pollution control technology

ABSTRACT: A method has been developed to delineate quantitatively waste concentrations throughout waste effluent mixing zones on the basis of densitometric measurements extracted from aerial photographs. A "mixing zone", as defined herein, is the extent of a receiving-water body utilized to dilute a waste discharge to a concentration characteristic of a totally mixed condition. Simultaneously-acquired color-infrared photographs and suspended solids water samples have been used quantitatively to delineate the mixing zone resulting from the discharge of a paper mill effluent at a study site within the state of Wisconsin. Digital scanning microdensitometer data were used to estimate and delineate suspended solids concentrations on the basis of a semi-empirical model. The results and experiences of the study have indicated that photographic photometry, if predicated on a limited amount of ground sampling, can be used to measure and delineate mixing-zone waste distributions as reliably and in more detail than conventional surface measuring techniques. The method has direct application to: (1) the establishment of definite and rational water quality guidelines; (2) the development of sampling and surveillance programs for use by governmental and private agencies; and (3) the development of design and location criteria for industrial and municipal waste effluent outfalls.

quality in the nation's surface waters. This lowering of environmental quality is a source of considerable public and governmental concern. This concern manifests itself, in a legislative sense, in the Federal Water Pollution Control Act Amendments of 1972 with the objective of restoring and maintaining the

coupled with a stable economic, social and political climate might make it possible to discharge no wastes into aquatic ecosystems at some time in the future, in the interim our finite aquatic ecosystems are having to bear the stress of various municipal and industrial waste discharges. Often neglected in the con-

trol of these pollution-laden discharges is the fact that their deleterious effect on their receiving water bodies is a strong function of how the waste effluents and receiving waters mix. For example, some discharges mix, and therefore dilute, quite rapidly in the receiving water. However, under some circumstances wastewater discharges can be devastating to a receiving water due principally to insufficient mixing and dilution.

Knowledge of the mechanisms by which pollutants are mixed and transported in natural river courses is implicit in the rational control of water quality. Unfortunately, this knowledge is sparse due in great part to the practical problems inherent in employing conventional techniques to measure physical parameters in *mixing zones*.

MIXING ZONE DEFINITION

If a pollutant is introduced into a river, the energy of the effluent discharge and that of the receiving water interact to disperse the pollutant, thereby reducing its concentration. This dispersal can be envisioned as a two-stage process. Immediately downstream from the point of discharge, the pollutant is dispersed by the interaction of the physical and flow characteristics of the effluent and outfall with those of the river. Further downstream, additional dispersal stems from the natural turbulence and velocity structure of the river. Dilution continues until the waste is totally mixed. The extent of the river over which this dilution takes place is herein defined as the *mixing zone*.

MIXING ZONE MODELING

During the past five years, an interdisciplinary research team at the University of Wisconsin has attempted to characterize the mixing zones at seven river discharge sites throughout the State of Wisconsin. Employing an integrated program of field sampling, mathematical modeling, laboratory modeling and remote sensing, this group has striven to develop a quantitative relationship for the volumetric configuration of the mixing zone as a function of the measurable characteristics of various effluents, outfalls, receiving water body characteristics and meteorological conditions. This predictive relationship would have value in: (1) the establishment of equitable and rational water quality guidelines; (2) the development of sampling and enforcement programs for government agencies; and (3) the development of design and location protocols for industrial and municipal outfalls. The general nature of this effort was reported by Villemonte *et al.*

(1973). It suffices to say here that the experiences of this endeavor have led to the conclusion that the extent, site dependence, spatial complexity and temporal dynamics that characterize the mixing zone make it impractical to model solely on the basis of conventionally collected field data. Consequently, remote sensing in the form of both aerial photography and thermal scanning has been invaluable in the modeling process.

An important part of the mixing-zone modeling progress to date has been the development of a methodology whereby densitometric data extracted from aerial photographs can be used quantitatively to estimate water quality parameters in mixing zones. This discussion treats the research effort leading to the development of this methodology. It entailed an extensive aerial and ground survey of a mixing zone resulting from the discharge of paper mill wastes at the Kimberly-Clark Paper Mill at Kimberly, Wisconsin. In the study, image optical densities extracted from color-infrared (CIR) transparencies were related to ground truth surficial suspended solids measurements, thereby enabling estimation of the parameters of a semi-empirical model. The model was subsequently used to delineate predicted solids concentrations throughout the mixing zone.

This presentation treats the salient characteristics, results, conclusions and recommendations of the Kimberly case study.* Preparatory to the description of the study is a discussion of the general nature and utility of mixing-zone photographs.

NATURE OF MIXING-ZONE PHOTOGRAPHY

PREVIOUS WORK

Research related to the aerial photographic study of mixing patterns has taken many forms during the past decade. Keller (1963) reported the experience of the Coast and Geodetic Survey in the photogrammetric determination of tidal currents. The Water Pollution Research Board of England (1964) described the photographic tracking of a sewage waste plume using drift poles and drogues. Romanovsky (1966) studied coastal waste diffusion by photographing dye release using a balloon. Ichiye and Plutchak (1966) performed photodensitometric measurements of ocean dye releases and related them to conventional fluorometric concentration measurements.

With the work of Scherz (1967) various

* The details of the research reported herein can be found in Lillesand (1973).

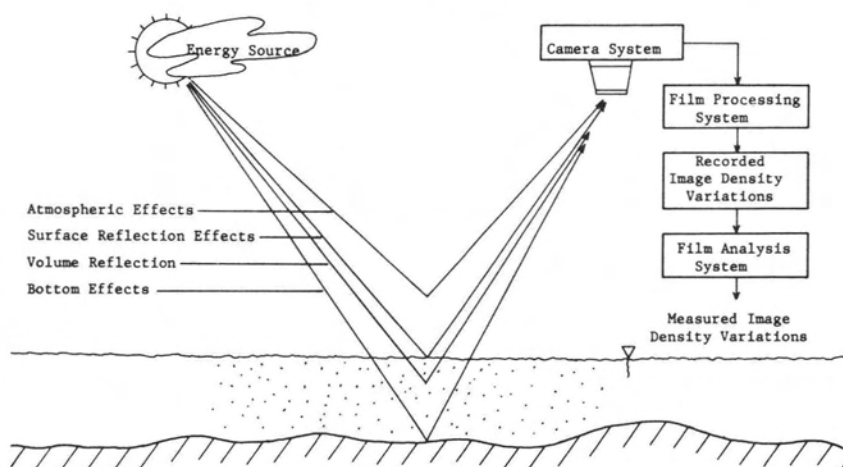


FIG. 1. Energy flow profile of airborne photographic mixing-zone monitoring system.

film-filter combinations began to be used to photograph waste plumes without the introduction of tracers. Scherz (1967), on the basis of laboratory spectroradiometric analysis of waste water samples, reported a correlation between water sample reflectance and waste concentration. Neumaier *et al.* (1967) identified industrial waste effluents on the basis of reflectance using photographs taken with submerged test panels present.

In work initiated in 1968, Burgess and James (1971) determined waste concentrations, water current patterns and diffusion coefficients near an ocean pulp mill outfall by relating photodensitometric measurements from multispectral photographs to conventional plume tracer data. Good correlation between the aerial and ground data was obtained. In fact, the comparison between the photographic concentration values as determined from film densities and ground truth was statistically better than the repeatability of the boat-sampling data.

Piech *et al.* (1969), Silvestro (1969), Piech and Walker (1971) and Scherz (1971) also presented the utility of relating photo image-density measurements to waste concentrations. At the same time, however, their work underscored the fact that image-density variations represent complex composite responses to which a number of factors might contribute. These factors and their relationship to quantitative estimation of mixing-zone water quality parameters are included in the following discussion.

COMPLEXITY OF PHOTOGRAPHIC RESPONSE

Photographic mixing-zone monitoring systems sense through two complex turbid

media, air and water, each of which has different properties. The flow of energy through these media is shown in Figure 1 wherein image formation is shown to be a function of: source effects (intensity and spectral distribution of sunlight and skylight); atmospheric effects (scatter and absorption); surface reflection effects (specular sunlight and skylight reflections); volume reflection effects (reflection from the pollutant and the polluted water); bottom effects (light returned from the bed of the receiving water body); camera system effects (geometric, photometric and mechanical operating characteristics); and film sensitometric effects (sensitivity, processing and handling). Finally, the energy-flow profile may be further confounded by the error effects associated with image-analysis procedures.

The possible complexity of this combination of factors influencing image formation in photographic mixing-zone monitoring systems must be recognized in assessing water quality on the basis of image-density measurement. Density variations recorded by film in response to changes in any energy-flow factor, or combination of factors other than volume reflectance, should not be interpreted as a manifestation of changes in water quality.

UTILITY OF PHOTOGRAPHIC RESPONSE

For typical *non thermal* effluent discharges, photo-image density measurements can be used quantitatively to predict water quality throughout the mixing zone if: (1) a systematic relationship is determined between water-sample reflectance and some measure of water quality (suspended solids,

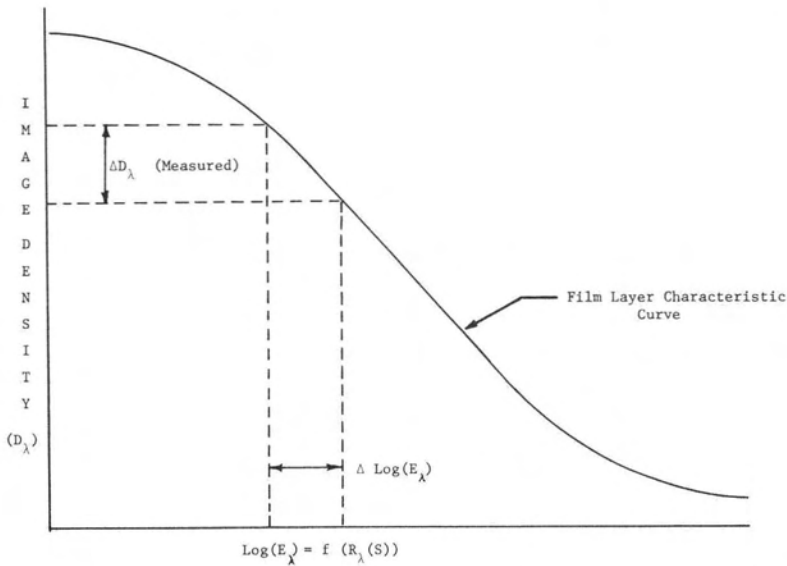


FIG. 2. Image-density/water-quality record typical of emulsion layer of a reversal film.

turbidity, etc.); (2) the relationship between film exposure and scene reflectance is accounted for; and (3) the relationship between film density and film exposure is adequately approximated. If these three criteria are met, measured image densities can be used to find film exposure levels; film exposure levels can be used to find scene reflectance levels; and scene reflectance levels can be used to predict water quality parameter values.

Figure 2 depicts the above described interplay between measured photo image density $\dagger D_\lambda$, film exposure E_λ , scene reflectance R_λ and a water quality parameter S . In interpreting this figure, it should be noted that only the relationship between image density and film exposure is shown explicitly. This relationship is embodied in the familiar characteristic D - $\log(E)$ curve. Shown in Figure 2 is the configuration of the characteristic curve typical of the emulsion layer of a reversal film.

The functional relationship between film exposure and scene reflectance stems from the theoretical calculation of irradiance in a camera focal plane as described by Jensen (1968), Piech and Walker (1971) and Lillesand (1973). Upon accounting for peripheral effects, it can be shown that film exposure at each point in the image plane is linearly dependent on scene reflectance.

The relationship between scene reflectance

\dagger The symbol λ is used throughout to indicate the wavelength dependence of the associated parameter.

and any given water quality parameter depends highly on the mixing-zone site and time of study. Once defined, however, it permits formulation of the mathematical configuration of a model indirectly relating image density to water quality. The parameters of the model can be estimated by relating limited ground truth, film sensitometry data and image density measurements. The resulting model can then be used to predict water quality values at arbitrary points in the mixing zone on the basis of image-density measurements.

The above process was employed to quantitatively delineate the Kimberly-Clark mixing zone by relating sensitometrically referenced photo densities to suspended solids concentrations.

KIMBERLY-CLARK CASE STUDY

BACKGROUND

Study Site. The Kimberly-Clark paper mill at Kimberly, Wisconsin is located on the Lower Fox River between Cedars Dam and Little Chute Dam. The general planimetric extent and configuration of the mixing zone indigenous to this site at the time of study is shown in Figure 3. The waste plume extended along the south shore of the river for nearly 1 mile before a totally-mixed condition was realized. This site was chosen for study on the basis of a number of factors. First, the waste character and river geometry present typified that of a number of mill sites within the State of Wisconsin. It was logisti-

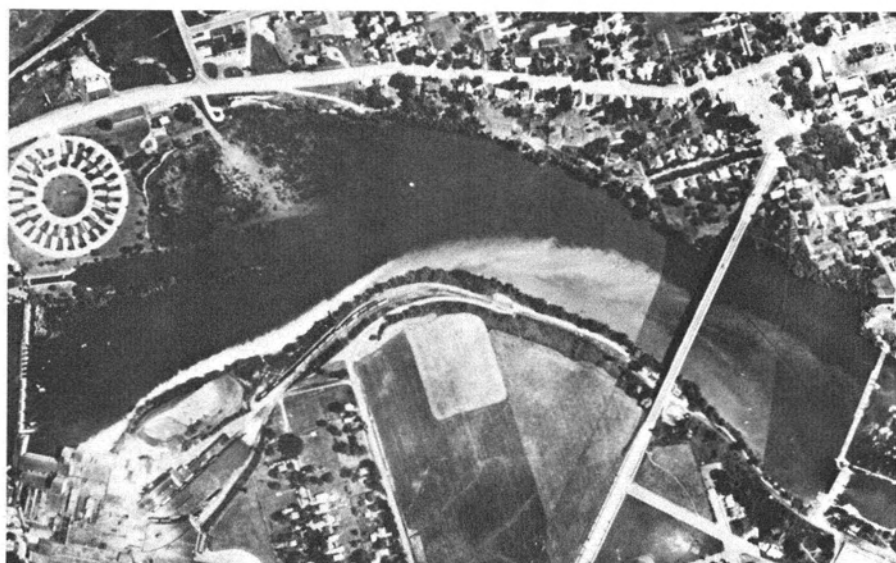


FIG. 3. Aerial photographic mosaic of the Kimberly-Clark Study area.

cally amenable to both aerial and ground observation. Mill management was interested in studying the mixing-zone conditions present prior to the installation of a new (currently operational) waste treatment facility. As will be described later, these factors were further complemented by the site's desirable vertical mixing characteristics and reflectance properties.

The waste field present at the site resulted from the discharge of paper production wastes at a rate of about 11 million gallons per day. The effluent was composed of titanium dioxide, aluminum hydroxide, wood fiber and process cooling water. The estimated BOD level of the waste amounted to 15,000 lbs. per day. The discharge of suspended solids was about 55,000 lbs. per day.

The effluent was discharged from a total of 21 outfalls located at the mill and along the south shore of the river. Four additional outfalls were located upstream from the plant. Nearly 70 percent of the total discharge was released from the main mill outfall. The discharge and velocity ratios (river to effluent) were about 120 and 0.20, respectively. Of particular interest in this discussion is the fact that Hoopes *et al.* (1973), on the basis of previous field studies, had drawn the following conclusions about the nature of the vertical mixing characteristics of the plume:

- Vertical stratification of the effluent near the plant was strong due to the blending of outfall discharges of different temperatures and flows.
- Beyond 400 to 500 ft from the plant the river

turbulence produced complete vertical mixing over the river depth (5-10 ft).

The latter mixing characteristic inferred that if the surficial waste concentration distribution of the mixing zone could be delineated, it would, to a great extent, reflect the volumetric distribution of the waste field as well. This made the site particularly amenable to photographic study.

In addition to desirable mixing characteristics, the site was found to offer a relatively uncomplicated relationship between water-sample waste concentration and sample reflectance. Laboratory spectroradiometric measurements conducted by Klooster and Scherz (1973) were found to demonstrate that water-sample reflectance was linearly related to sample turbidity and suspended solids over the range of 0-200 mg/l. Knowledge of this linear dependency facilitated the formulation of the mathematical configuration of a model for the site that related photo image densities and suspended solids concentrations.

Development of Suspended Solids/Density Model. From the above reflectance analyses, it was shown that water-sample reflectance could be related to suspended solids concentration in accordance with

$$R_{\lambda} = K_1(\lambda) S + K_2(\lambda) \quad (1)$$

where R_{λ} is the water sample reflectance, S is the concentration of suspended solids, and $K_1(\lambda)$ and $K_2(\lambda)$ are parameters describing linearity.

As indicated earlier in this discussion, film exposure can be linearly related to scene re-

flectance. This relationship can be expressed as

$$E_{\lambda} = K_3(\lambda) R + K_4(\lambda) \quad (2)$$

where E_{λ} is the film exposure and $K_3(\lambda)$ and $K_4(\lambda)$ are parameters of linearity.

The characteristic, or D - $\log(E)$, curve for a given analysis wavelength can be derived from densitometric film processing control data. Characteristic curves vary between film types, between films of the same time, and between layers of the same film. For common reversal film, however, the general configuration of the curve has been shown by Dana (1973) to be closely approximated by

$$D_{\lambda} = B_0(\lambda) + B_1(\lambda) Z_{\lambda} + B_2(\lambda) Z_{\lambda}^2 + B_3(\lambda) Z_{\lambda}^3 \quad (3)$$

where D_{λ} is the film density, Z_{λ} is equal to relative $\log(E_{\lambda})$ and $B_0(\lambda)$, $B_1(\lambda)$, $B_2(\lambda)$ and $B_3(\lambda)$ are parameters expressing the configuration of the characteristic curve for a given wavelength of analysis.

Equations 1 through 3 permit the development of a model which provides for the estimation of suspended solids S , from measured image density D_{λ} , such that

$$S = \alpha_{\lambda} \cdot 10^{Z_{\lambda}(D_{\lambda})} + \beta_{\lambda} \quad (4)$$

where α_{λ} and β_{λ} are model parameters.

Equation 4 will hereafter be referred to in this discussion as the Suspended Solids/Density model; or simply the SSD model.

Study Intent. If the SSD model including its associated assumptions, as more fully detailed by Lillesand (1973), could be used to provide reliable suspended-solids concentration predictions on the basis of photodensitometric measurement, it would greatly enhance the mixing-zone modeling process. The primary goal of the Kimberly study was to evaluate, in the context of mixing-zone modeling, the utility of the SSD model. The data acquisition scheme employed in the study was designed to provide a means of comparing a conventional ground delineation of the mixing zone to a photographically derived rendition. Accordingly, the field activities performed during the study, in the summer of 1972, entailed the simultaneous acquisition of substantial amounts of aerial photographic and ground truth data. Densitometric image measurement completed the data-acquisition endeavors of the study. The procedures employed to collect the ground truth, aerial photography and image density information are the subject of immediate attention. Subsequent discussion will treat the procedures used to employ these data in the implementation of the SSD model.

DATA ACQUISITION

Ground Truth. During the course of a 1½-hour time period, ground crews acquired surficial (top 6 inches) suspended-solids samples at a total of 82 sampling positions throughout the plume. This effort entailed the use of two identically equipped boats, the positions of which were determined by theodolite tracking from shore. Sampling points were generally located along a series of 17 boat transects normal to the longitudinal axis of the plume. Shown in Figure 4 is the general location of the 17 transects as well as the location of the survey stations used in the theodolite tracking endeavor.

Sampling within any given transect included samples acquired both inside and outside of the plume. The number of sample points in any given transect varied from 3 to 10 in accordance with the width of the plume at the particular transect location. The time between occupation of successive sample points ranged from 30 seconds to 1 minute. In each transect at least one replicate, or repeated, water sample was acquired. This entailed duplicate sample collection as proximate in time and location as possible. This was done to permit the estimation of the experimental error inherent in collecting and analyzing a given water sample.

Within six hours from the time of acquisition, water samples were transported from the field to a cold-storage environment. Suspended solids analyses were subsequently conducted in accordance with the standard filtering and gravimetric methods described in American Public . . . (1971). Again, to estimate experimental error, random samples were split and analyzed independently during the laboratory analysis procedure.

Aerial Photography. Nearly continuous, vertical photographic coverage complemented the ground-truth activities. Primary photographic coverage took the form of 9-inch format CIR transparencies (Kodak Type 8443; Zeiss B minus blue filter). Average scale of the photographs was 333 feet per inch. Film exposure conditions departed from those typical of conventional mapping photography in terms of time of photo acquisition. Photography commenced at 14:30 hr (CST). The low solar altitude associated with this time eliminated direct sunlight surface reflections from the imagery.

Prior to processing the film, a 21-step calibration wedge was contact printed on the unexposed film leader. The source light/filter combination used in this endeavor was chosen to duplicate as nearly as possible the conditions under which the film was exposed

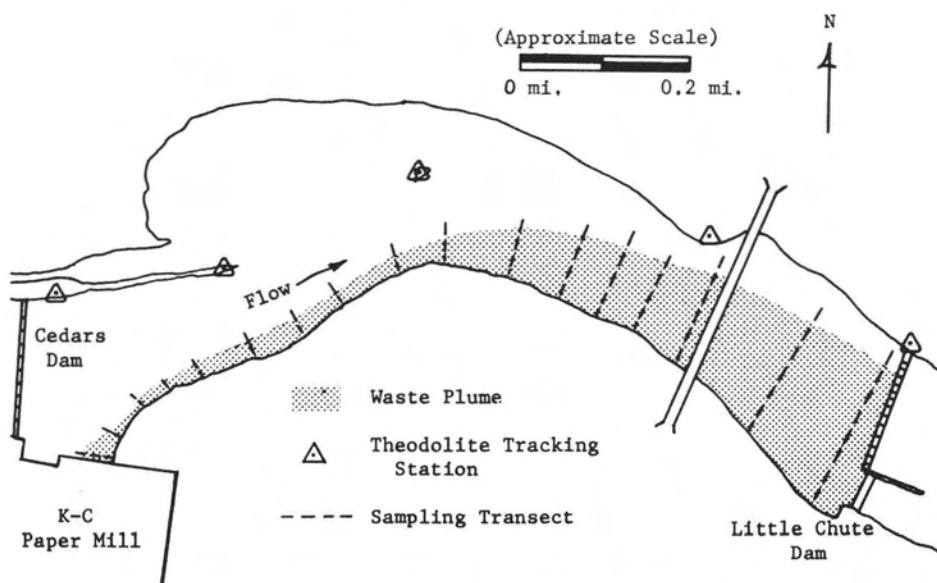


FIG. 4. Location of boat sampling transects and shore theodolite tracking stations.

in the field. The resulting step wedge image provided a reliable means of preparing the characteristic curves for the film.

The film was commercially processed in Kodak EA-5 processing chemistry. In order to increase the photographic detail of the waste field images, the film was somewhat *force processed*. Prior to the development of the entire film roll, two test exposures were processed under typical and slightly elevated temperature conditions, respectively. Adequate plume detail was realized only under the latter process condition. Processing the entire roll under this condition resulted in an enhanced display of densities in the imagery of the effluent plumes, and a corresponding degradation of detail in images of surrounding land features.

Metric reduction of the photographs entailed computation of sample-point object-space positions from the shore theodolite data, followed by a two-dimensional conformal coordinate transformation under the assumption of verticality. Images of at least three and as many as seven pre-paneled ground control points appeared in each photo permitting least squares estimation of transformation factors. These transformation factors were then used to compute the photo coordinates of ground sampling points appearing in each frame. This process provided the geometric means of relating subsequent image density measurements to the respective ground-truth measurements.

Microdensitometry. Preliminary densitometry of a total of 29 photos imaging the

ground sampling points was performed using a spot microdensitometer equipped with a monochromator. This technique was used to isolate seven discrete analysis wavelengths at each sample point. These analysis wavelengths ranged from 0.4 to 0.7 μm in increments of 0.05 μm . Density measurement at the precise ground sample point positions was quite awkward because the spot densitometer system used did not provide for convenient spatial reference of the image measurement position to the photo fiducial axis system. Resulting geometric errors were also compounded by the radiometric instability of the densitometric system. This was due to variations in light-source intensity, changes in light-source spectral character, lack of image plane flatness and disturbance of the system's optical train alignment. Despite these geometric and radiometric limitations, however, the spot densitometric analysis procedure did permit the typification of the spectral film response curves for the waste effluent and its background receiving water.

Film response curves (density vs. wavelength) were prepared for all sample points. The general configuration of these curves was essentially constant and there was a general systematic suppression of density (at all wavelengths) associated with increased waste concentration. This meant that from the standpoint of film response, it made little difference where one *looked* spectrally to evaluate the relationship between density and solids concentration. On this basis, final

densitometry took the form of broad-band integration of the film-density responses in each of the three film layers.

In order to extract density readings having increased geometric and radiometric integrity, an automated digital scanning microdensitometer system was employed during final densitometric analysis. The anticipated expense of acquiring, manipulating and analyzing the digital scanning data led to a decision to limit final analysis to a thorough study of but five photos. The photos chosen for analysis were those that collectively imaged the entire waste field and also minimized the differences in time of acquisition between the photos themselves and the ground samples included in their respective coverage areas.

Each of the analysis photos as well as the film step-wedge image was scanned three times. In this effort, the source light was filtered in each of three broad wavelength bands which isolated the blue-forming, green-forming and red-forming layers of the CIR emulsion. The filters used were Wratten number 47, number 58 and number 24 for the blue, green and red layers, respectively. A scanning aperture and scan line spacing of $100\mu\text{m}$ was used; thus yielding 250 density observations per lineal inch along a scan line, or 62,500 observations for a 1-inch square film area. This scanning configuration resulted in taking density readings in 256 gray levels over areas of the film imaging contiguous ground areas approximately 1.33 ft square. These readings, being in a digital form and being recorded on magnetic tape, were amenable to a number of forms of manipulation, display and analysis. Their use in the implementation of the SSD model is described below.

IMPLEMENTATION OF THE SUSPENDED SOLIDS/DENSITY MODEL

Implementation of the SSD model rudimentarily entailed relating the digital density data extracted at each ground truth sample point to its associated suspended solids concentration in accordance with

$$S = \alpha_{\lambda} \cdot 10^{Z_{\lambda}(D_{\lambda})} + \beta_{\lambda} \quad (5)$$

(Equation 5 is the form of the SSD model as developed in Equation 4; it is repeated here for convenience.)

The model was *calibrated* for each of the three film layers on the basis of the 82 observations of density D_{λ} and suspended solids S . This calibration took the form of a least-squares solution for the unknown model parameters α_{λ} and β_{λ} . The computational sequence was initiated by solving for the log

exposure Z_{λ} associated with each density observation D_{λ} . This was accomplished by finding Z_{λ} as a function of D_{λ} on the basis of a cubic approximation to the characteristic curve for each film layer. Knowledge of Z_{λ} for each D_{λ} enabled the least-squares solution for α_{λ} and β_{λ} . This provided the means for using the model to measure suspended solids concentrations at arbitrary points in the mixing zone solely on the basis of film-density measurement.

It should be noted that although the above description of the model implementation procedure is entirely accurate, it has been somewhat simplified in the interest of clarity. First of all, it presupposes the determination of the cubic polynomial approximating the D -log(E) curve for each film layer. Secondly, it evades the fact that the SSD model was derived under the assumption of a single point in time, under a single set of prevailing observational conditions. As applied herein, the model was used in the analysis of density data extracted from five photographs which were taken over the course of a 70-minute time period. For this reason, density observations had to be normalized before the model could be implemented.

The intent of the immediate discussion is to detail the methods and results of (1) approximating the D -log(E) curve for each film layer with cubic polynomials; (2) normalizing image densities to account for differences in observational conditions between photographs; and (3) estimating the unknown model parameters of the SSD model for each film layer.

Characteristic Curve Approximation. The characteristic curve for each film layer was approximated by relating the density measured at each step of the step tablet image to the relative log-exposure associated with each step. The limits of this approximation were chosen to concur with the extremes of the density ranges recorded on the analysis photos in each wavelength. These limits were defined by the 7th and 15th step of the calibration wedge where relative log(E), or Z , values were 0.87 and 2.09, respectively. Each of the three curves were fit, over this range, with third-order polynomials of the form

$$D_{\lambda} = B_0(\lambda) + B_1(\lambda)Z + B_2(\lambda)Z^2 + B_3(\lambda)Z^3 \quad (6)$$

where the parameters $B_0(\lambda)$, $B_1(\lambda)$, $B_2(\lambda)$ and $B_3(\lambda)$ were constant for any film layer. Having nine observations of density and relative log-exposure Z enabled a least-squares solution for these parameters. The resulting values for $B_0(\lambda)$, $B_1(\lambda)$, $B_2(\lambda)$ and $B_3(\lambda)$ are summarized for each film layer in Table 1.

TABLE 1. SUMMARY OF PARAMETERS OF CUBIC POLYNOMIALS USED TO APPROXIMATE CHARACTERISTIC CURVES

| Parameter | Layer | | |
|----------------|-------------|-------------|-------------|
| | Blue | Green | Red |
| $B_0(\lambda)$ | 9.172 | 2.478 | 1.672 |
| $B_1(\lambda)$ | -12.258 | 1.458 | 4.606 |
| $B_2(\lambda)$ | 5.766 | -2.661 | -5.526 |
| $B_3(\lambda)$ | -0.919 | 0.722 | 1.436 |
| $s_o(\lambda)$ | ± 0.035 | ± 0.030 | ± 0.055 |

The standard deviations of unit weight s_o associated with each of the three solutions are also given in Table 1.

The graphic relationship that the various approximating polynomials bore to the actual observations used to derive them is typified by Figure 5 which shows the cubic approximation to observations extracted from the red film layer.

Density Normalization. The five analysis photos were acquired over a span of about 70 minutes. During this time period film exposure magnitudes naturally changed in response to changes in scene illuminance. Density observations were normalized to account for these changes as well as any format-related variations (optical fall-off, etc.) the imagery may have held. In this effort, the average density of the receiving water outside of the waste plume was used as a computational reference between photos. The average background water density on the photo taken earliest was chosen as the base value to which the background water reference den-

sities on the remaining photos were normalized. Computation of the density differences (and log-exposure differences) between the background water on the first photo and on the subsequent photos enabled correction of the densities measured at sample points within the plume. Choice of the background water as a standard of reference for density normalization was made on the basis of convenience. It was a standard of reference that appeared on each analysis frame in the area of sampling. Implicit in its use was the assumption that the background water did not change in character during the time of photography or over the area of interest. There were no changes in prevailing river conditions noted during the time of observation that would tend to invalidate this assumption.

The computational sequence used to normalize the sample point densities can best be understood with reference to Figure 6. This sequence was initiated with solution for the relative log-exposure $Z_R(\lambda)$ for the background water on the master reference photo. This amounted to solving the appropriate characteristic-curve approximating equation for $Z_R(\lambda)$ in terms of the measured background water density $D_R(\lambda)$. Similar solution was performed for the relative log-exposure $Z_N(\lambda)$ for the background water on each of the four photos to be normalized. This was done on the basis of the background water density $D_N(\lambda)$ measured on each photo. The change in scene exposure ΔZ_λ was computed from

$$\Delta Z_\lambda = Z_R(\lambda) - Z_N(\lambda). \tag{7}$$

The unrefined relative log-exposure $Z_P(\lambda)$ for

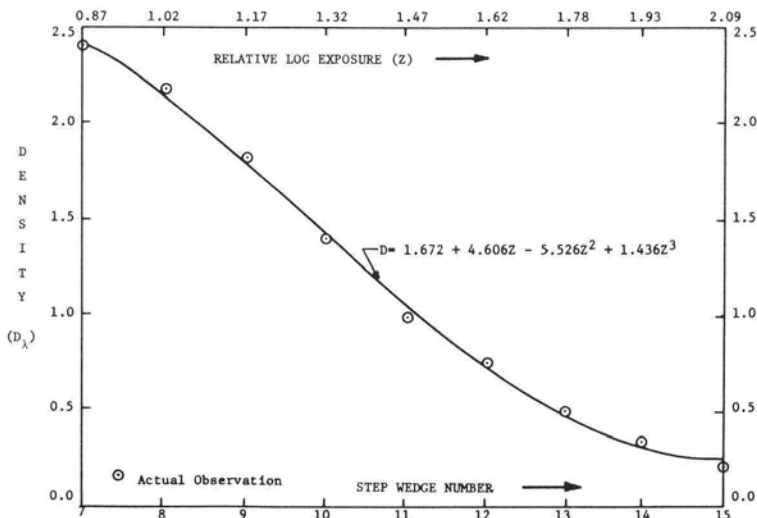


FIG. 5. Cubic polynomial approximating characteristic curve of red film layer.

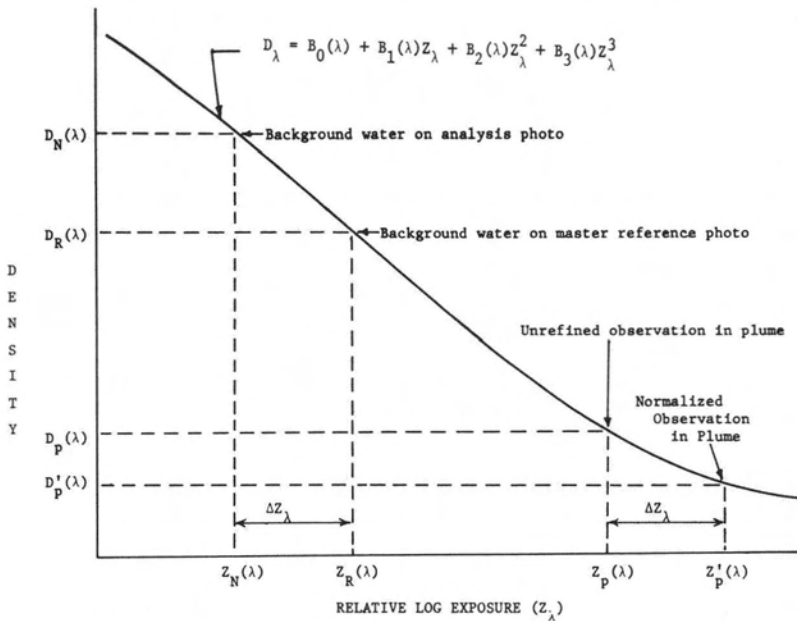


FIG. 6. Computational elements of density normalization.

points in the plume was computed (from the appropriate polynomial) on the basis of the unrefined density measurements $D_P(\lambda)$ at each sample point. Thereafter the normalized relative log-exposure $Z'_P(\lambda)$ for each sample point was computed from

$$Z'_P(\lambda) = Z_P(\lambda) + \Delta Z_\lambda \quad (8)$$

Finally, the normalized densities $D'_P(\lambda)$ for each analysis point was found on the basis of solving the characteristic-curve function for each $Z'_P(\lambda)$. These normalized densities were then used along with the suspended solids data to estimate the parameters of the SSD model for each film layer.

Model Parameter Estimation. The normalized densities and their related suspended solids measurements were used to solve for the unknown model parameters (α_λ and β_λ) associated with each of the three film layers. This entailed a least-squares solution of 82 observation equations of the form

$$S_n = \alpha_\lambda 10^{Z_{\lambda,n}(D_{\lambda,n})} + \beta_\lambda + v_{\lambda,n} \quad (9)$$

where $v_{\lambda,n}$ represents the residual associated with the n th suspended solids observation.

For each normalized density measurement, the corresponding relative log-exposure $Z_\lambda(D_\lambda)$ was computed from the appropriate cubic characteristic-curve approximating relationship. Having these values, the values for exposure $10^{Z_\lambda(D_\lambda)}$ were computed and a matrix solution for the unknowns was performed. The results from applying this solution procedure to each film

TABLE 2. SUMMARY OF PARAMETERS COMPUTED IN THE IMPLEMENTATION OF THE SUSPENDED SOLIDS/DENSITY MODEL

| Parameter | Blue | Layer Green | Red |
|-----------|---------|----------------|---------|
| α | 1.703 | 1.886 | 1.725 |
| β | -16.708 | -15.052 | -13.165 |

layer are summarized in Table 2. The graphical relationship that the various models bore to the observed density/solids data used to develop them is typified by Figure 7. This figure shows the results of model solution for the red film layer.

In evaluating the solution of the various model parameters it was noted that the distribution of the input data was far from ideal. The majority of observations clustered at levels of high density and low concentration. This data distribution reflected the geographic distribution of solids within the waste plume. It was initially thought that a more statistically reliable solution for the model parameters might have resulted if an effort had been made to collect ground truth more uniformly over the range of concentrations rather than on a uniform geographic basis. Also, plume changes between the time of photography and time of water-sample acquisition could not be accounted for in the input data. The geometric errors inherent in

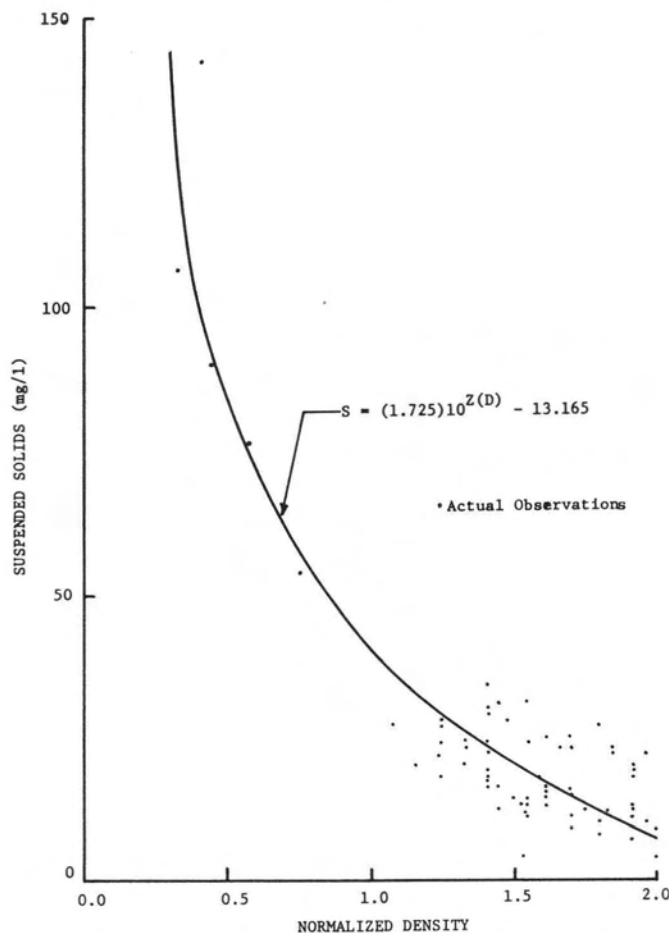


FIG. 7. Suspended-solids/density model of red film layer.

relating density measurements to ground measurements could have also degraded the input data.

In closing this portion of the discussion, however, it should be noted that *an adequacy of fit test performed on each model solution showed variations between observed and modeled concentrations to be attributable to the experimental error inherent in collecting and processing the suspended solids ground truth.* (This error was estimated from the variance associated with the aforementioned replicate samples.) On this basis the SSD model was used in the prediction and delineation of solids concentrations through the mixing zone.

MIXING-ZONE DELINEATION

The SSD model for each film layer was used to prepare a quantitative delineation of concentrations on a digital-density computer

printout of each of the analysis photos. The delineation technique amounted to computing and coding the densities associated with concentrations in excess of 10 mg/l (in 10 mg/l increments) throughout the plume. The computational elements of this procedure entailed an *inverse* or *back* solution of the SSD model.

Starting with the basic model form

$$S = \alpha_{\lambda} 10^{Z(D_{\lambda})} + \beta_{\lambda}$$

rearranging,

$$10^{Z(D_{\lambda})} = (S - \beta_{\lambda}) / \alpha_{\lambda}$$

from which

$$Z(D_{\lambda}) = \log((S - \beta_{\lambda}) / \alpha_{\lambda}) \quad (10)$$

Equation 10 was used to solve for the normalized relative log-exposure $Z(D_{\lambda})$ associated with each concentration S . Knowing $Z(D_{\lambda})$ for each concentration, solution for the related normalized image density D_{λ} was accomplished through

$$D_{\lambda} = B_0(\lambda) + B_1(\lambda) Z_{\lambda} + B_2(\lambda) Z_{\lambda}^2 + B_3(\lambda) Z_{\lambda}^3$$

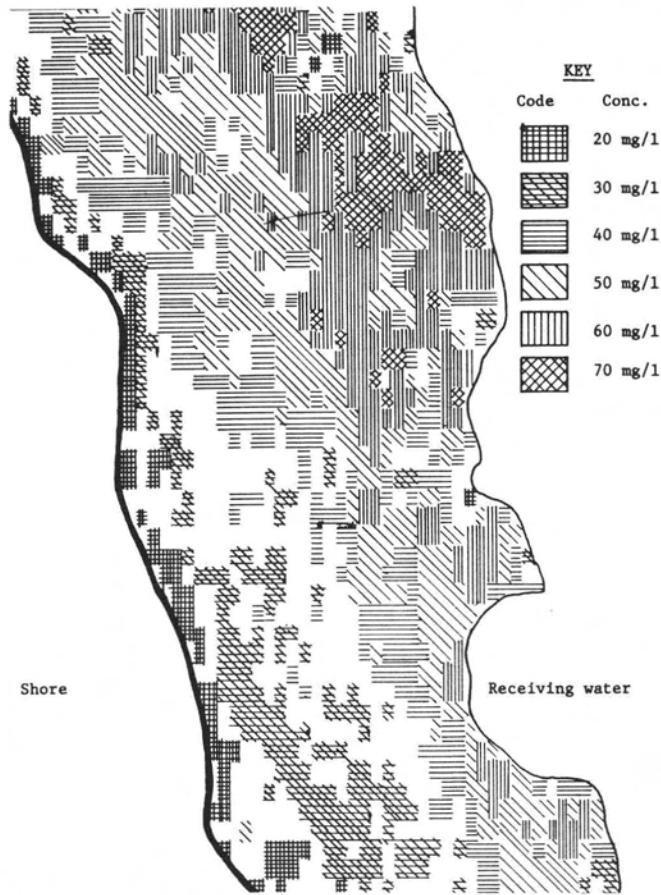


FIG. 8. Portion of equal concentration delineation obtained from red film layer.

Finally, the uncorrected density associated with each normalized density was found by the reversal of the density-normalization process.

After the densities related to each concentration were determined, delineation amounted simply to coding all image areas where these densities occurred. Figure 8 is a small portion of the equal concentration delineation obtained in the red film layer.

Space necessarily precludes inclusion herein of more demonstrative computer generated delineations. A future publication will detail the results of applying various computer delineating methodologies to the SSD model data. Of interest in the remaining portion of this discussion are the conclusions and recommendations related to the model's utility in the Kimberly case study in particular and the mixing zone modeling process in general.

CONCLUSIONS AND RECOMMENDATIONS

CONCLUSIONS

Based on the results and experiences of the research reported herein and studies preliminary thereto, the following conclusions have been drawn:

- Reliable mixing-zone modeling solely on the basis of conventionally collected field data is virtually impossible in light of the extent, spatial complexity and temporal dynamics that characterize the mixing zone.
- Photodensitometric measurements, coupled with ground truth and analyzed with due regard for peripheral effects can be used reliably to predict the level of water quality parameters in the mixing zone.
- The suspended solids/density model as developed and implemented in the Kimberly-Clark case study has been used to delineate surficial suspended-solids concentrations as reliably and in more detail

than conventional surface-measuring techniques.

RECOMMENDATIONS

The photodensitometric method of waste concentration embodied in the development and implementation of the SSD model should be tested and refined at various sites, characterized by different types of effluents and different sets of observational conditions. In this regard it is suggested that:

- ★ Laboratory and/or field spectroradiometric analyses be performed for each site in order to account for the mathematical configuration of the water quality configuration/reflectance relationship indigenous to the site. This will dictate the number of model parameters to be estimated and the consequent statistical design of the ground-truth acquisition activities.
- ★ The spectroradiometric reflectance analyses should serve as a guide to the selection of the emulsion type to be used for the aerial photographic coverage. For example, black-and-white photography might be the best and most economical way of acquiring the photometric estimate of concentrations. The use of narrow-band filtration should be evaluated. In order to put all ranges of scene exposure into the linear section of a film response curve, multi-camera blanks might be used, each camera containing the same emulsion but set for different, yet simultaneous, exposures.
- ★ The indirect relationship that water-sample reflectance might bear to all important measures of water quality should be considered. Establishment of such relationships might permit photodensitometric quantification of certain parameters which do not alter the photographic properties of a water body directly.
- ★ Every effort should be made to evaluate the *truth* of the ground truth. Adequate estimation of the precision, accuracy and spatial representation of water quality measurements acquired in each mixing must be provided for.
- ★ Alternative methods for delineating and displaying water quality parameter distributions derived from density data should be investigated. In addition to conventional computer coding of digital scanning microdensitometer data, these methods might range from totally photographic *equidensity film enhancement* as described by Nielsen (1972), to color coded displays on electronic image analyzers. The great advantage to the latter two techniques is the elimination of the need to measure, store, retrieve and redisplay the mass of digital data associated with the scanning microdensitometer technique.

In closing, it is suggested that the results and experiences of this research, and those of related ongoing and future research assist in:

- The establishment of flight planning, film calibration and film processing guidelines for the acquisition of water quality photography to be used for quantitative purposes.
- The expeditious hydrodynamic modeling of the mixing zone in order to formulate outfall structure design and location protocols.
- The practical implementation of photographic water quality enforcement procedures.
- The development and updating of rational, definite and equitable water quality guidelines in general and *zone-of-passage* guidelines in particular. These guidelines should provide for criteria which, from the standpoint of practical enforcement, are amenable to symoptic remote sensing surveillance. These might include additional new measures of water quality, more readily extractable from aerial data than existing parameters, more reliable than these parameters and more representative than these parameters.

ACKNOWLEDGMENTS

This work was sponsored by the National Aeronautics and Space Administration Office of University Affairs (Grant No. NGL 50-002-127) and the Department of Natural Resources of the State of Wisconsin.

Prof. John A. Hoopes and Prof. James R. Villemonte, Department of Civil and Environmental Engineering at the University of Wisconsin, Madison, have initiated and directed the interdisciplinary mixing-zone modeling program of which this study was a part. Prof. James P. Scherz directed the laboratory reflectance analyses.

The Institute for Environmental Studies and the Engineering Experiment Station of the University of Wisconsin, Madison, have provided the administrative support for this study.

The cooperation and support of the Kimberly-Clark Corporation in this study was invaluable.

The success of this study was predicated on the able assistance of a number of students who provided able assistance in the gathering of field measurements, reduction of field data and in the performance of laboratory analyses. Mr. William L. Johnson is particularly acknowledged for his participation in these activities.

REFERENCES AND BIBLIOGRAPHY

- American Public Health Association, AWWA, *Standard Methods for the Examination of Water and Wastewater*, 13th ed., 1971.
- Burgess, Fred J., and James, Wesley P., "Airphoto Analysis of Ocean Outfall Dispersion", *Water Pollution Control Research Series*, No. 16070, Environmental Protection Agency, 1971.
- Dana, R.W., "Digital Sensitometry of Color Infrared Film as an Aid to Pattern Recognition Studies", *Proceedings*, 2nd Annual Remote Sensing of Earth Resources Conference, Tulsa, Oklahoma, Tennessee, March, 1973.
- Hoopes, John A., Villemonte, James R., Wu, Dong S., and Lillesand, Thomas M., "Mixing Zone Studies of the Wastewater Discharge from the Kimberly-Clark Paper Mill into the Fox River at Kimberly, Wisconsin", Report to State of Wisconsin Department of Natural Resources, 1973.
- Ichiye, T., and Plutchak, N.B., "Photodensitometric Measurements of Dye Concentration in the Ocean", *Limnology and Oceanography*, 1966.
- Jensen, Niels, *Optical and Photographic Reconnaissance Systems*, John Wiley and Sons, Inc., 1968.
- Keller, Morton, "Tidal Current Surveys by Photogrammetric Methods," U.S. Coast and Geodetic Survey, *Technical Bulletin* 32, 1963.
- Klooster, Steven A., and Scherz, James P., "Water Quality Determination by Photographic Analysis", *Proceedings*, 2nd Annual Remote Sensing of Earth Resources Conference, Tulsa, Oklahoma, Tennessee, March, 1973.
- Lillesand, Thomas M., "Use of Aerial Photography to Quantitatively Estimate Water Quality Parameters in Surface Water Mixing Zones", Ph.D. Thesis, University of Wisconsin, Madison, Wisconsin, 1973.
- Neumaier, G., Silvestro, F., Thung, H., and Frank, R., "Project AQUA-MAP Development of Aerial Photography as an Aid to Water Quality Management", *Cornell Aeronautical Laboratory Report*, Contract HC-9768, 1967.
- Nielsen, U., "Agfacontour Film for Interpretation", *Photogrammetric Engineering*, 38 (11): 1099-1105, November, 1972.
- Piech, Kenneth R., Silvestro, F.B., and Gray, R.J., "Industrial Effluent Diffusion in Rivers: A New Approach to Theory and Measurement", *Proceedings*, Conference of the Institute of Environmental Sciences, Anaheim, California, April, 1969.
- Piech, Kenneth R., and Walker, J.E., "Photographic Analyses of Water Resource Color and Quality", *Proceedings*, 37th Meeting of American Society of Photogrammetry, Washington, D.C., March, 1971.
- Romanovsky, V., "Coastal Currents", *Proceedings*, 3rd International Conference on Advances in Water Pollution Research, Munich, 1966.
- Scherz, James P., "Aerial Photographic Techniques in Pollution Detection", Ph.D. Thesis, University of Wisconsin, Madison, Wisconsin, 1967.
- Scherz, James P., "Monitoring Water Pollution by Remote Sensing", *Journal of the Surveying and Mapping Division*, American Society of Civil Engineers, November, 1971.
- Silvestro, Frank B., "Quantitative Remote Sensing of Water Pollution", *Proceedings*, Conference of the Institute of Environmental Sciences, Anaheim, California, April, 1969.
- Villemonte, J.R., Hoopes, J.A., Wu, D.S., and Lillesand, T.M., "Remote Sensing in the Mixing Zone", *Proceedings*, International Symposium on Remote Sensing of Water Resources, Burlington, Ontario, Canada, June, 1973.
- Water Pollution Research Board, "Report of the Director, Department of Scientific and Industrial Research", London, 1964.

Articles for Next Month

- Arthur T. Anderson, First ERTS-1 Mosaic of the U.S.
- James M. Anderson, ISP Commission III Symposium.
- Michael C. Y. Hou, Are Three Pointings Necessary?
- V. Klemas, D. Bartlett, & R. Rogers, Coastal Zone Classification from Satellite Imagery.
- Ross W. Leamer, Daniel A. Weber, & Craig L. Wiegand, Pattern Recognition of Soils and Crops from Space.
- Harold E. Lockwood & Dr. Gerard E. Sauer, Processing Corrections for Skylab Photographic Imagery.
- Robert B. McEwen & James W. Schoonmaker, Jr., ERTS Color Image Maps.
- Joseph J. Ulliman, Cost of Aerial Photography.
- Bruce C. Forster, Aerotriangulation Accuracy.
- Brian J. Myers, Rock Outcrops Beneath Trees.
-